

DYNAMIC RESPONSE ANALYSIS OF FOUR-SIDE SUPPORTED RC SLABS UNDER IMPACT LOADING

Dandan ZHENG^{*1}, Masato KOMURO^{*2}, Norimitsu KISHI^{*3} and Tomoki KAWARAI^{*4}

ABSTRACT

In this study, 3D elasto-plastic dynamic response analyses for four-side rectangular reinforced concrete slabs under impact loading were conducted. An analytical method with erosion technique was proposed, and its applicability was investigated comparing with the experimental results under various impact velocities. The results obtained from this study were as follows: 1) configurations of time histories of the impact force, the reaction force, and the deflection of the lower surface at the loading point can be better predicted for all cases; 2) crack patterns can be better evaluated using the proposed method.

Keywords: four-side supported RC slabs, finite element analysis, impact loading, erosion technique

1. INTRODUCTION

Over the past few decades, in the mountainous areas and coastlines in Japan, many rockfall protection structures have been constructed to protect transportation networks and human lives from falling rocks. Due to the natural disasters such as mud-rock flow, rockfall, and earthquake, the number of damage events on rockfall protection structures such as reinforced concrete (RC) rock-sheds, retaining walls, steel wire nets, and fences has been increased. To establish the reasonable design method for impact resistant RC structures such as rock protection gallery, a large number of impact tests were conducted using prototype rock-sheds and small-scale RC slabs [1-3]. Meanwhile, to achieve this goal more efficiently, the numerical analysis studies should be conducted to save the time and cost also.

It is shown that impact response behaviors of RC slabs without punching shear failure under low-speed impact loading can be better simulated using numerical analysis method proposed by previous studies [4]. However, it is found that in the case of RC slab with punching shear failure, impact response behavior of the slab was underestimated by using this method because punching shear cracks may not be properly evaluated. Therefore, it is more important and imminent to establish a reasonable numerical simulation method for analyzing punching shear failure behaviors of RC slabs under low-speed impact loading.

Here, in this study, to establish the reasonable numerical analysis method for rectangular RC slab under low-speed impact loading, 3D elasto-plastic dynamic response analyses with erosion technique were conducted for the slabs with punching shear failure. The applicability of the proposed analysis method was

verified comparing with the experimental results [2]. Here, LS-DYNA commercial program (ver. R9) was used.

2. OUTLINE OF EXPERIMENTS

2.1 Dimensions of RC slabs

Figure 1 shows the dimensions and reinforcement layouts of the rectangular RC slabs used in this study, which is modelled the roof slab of actual RC protection galleries. Dimensions of the slabs were 2,000 × 2,000 × 210 mm (width × length × depth). The slab was four-side

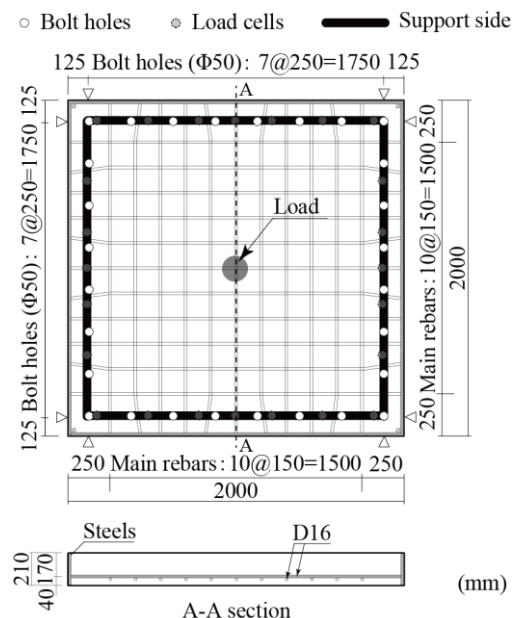


Fig. 1 Dimensions and reinforcement layouts of rectangular RC slabs

*1 Ph.D. Student, Division of Engineering, Muroran Institute of Technology, JCI Student Member
 *2 Associate Prof., Dept. of Civil Engineering, Muroran Institute of Technology, Dr. E., JCI Member
 *3 Specially-Appointed Prof., Muroran Institute of Technology, Dr. E., JCI Member
 *4 Ph.D. Student, Division of Engineering, Muroran Institute of Technology, JCI Student Member

Table 1 Mechanical properties of concrete

Compressive strength f'_c (MPa)	Tensile strength f_t (MPa)	Elastic modulus E_c (GPa)	Poisson's ratio ν_c
28.9	2.89	19.26	0.167

Table 2 Mechanical properties of rebars

Type	Yield strength f_y (MPa)	Elastic modulus E_s (GPa)	Poisson's ratio ν_s
D16	389	206	0.3

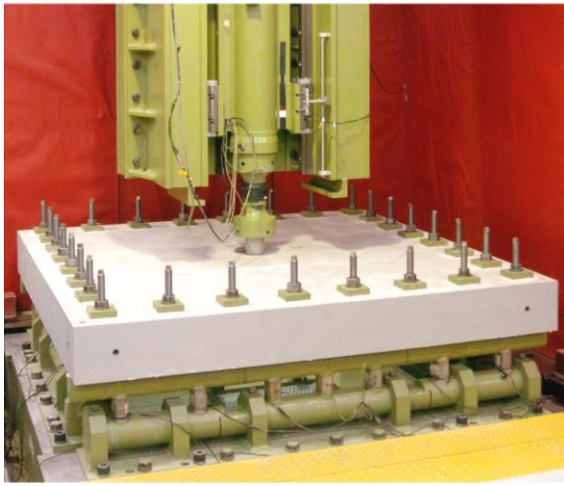


Photo. 1 Experiment setup

supported and both clear spans were 1,750 mm. Deformed rebars of diameter $\phi = 16$ mm were placed every 150 mm in two directions, and the average depth of concrete cover was 40 mm. The rebar ratio of the specimen was about 0.9 %. And the main rebars were welded to the anchor plate having $t = 7$ mm thickness at the end of slab to save the anchorage length.

Table 1 and 2 show the material properties of concrete and main rebars. The compressive strength of concrete f'_c , and yield strength of reinforcing bars f_y are obtained from the material tests conducted. Poisson's ratio of concrete ν_c , the elastic modulus of rebars E_s and Poisson's ratio of reinforcing bars ν_s were assumed to be nominal values.

2.2 Experimental procedure and measuring items

Photo 1 shows the experimental setup on four-side supported RC slab. In the experiment, a single impact load method was applied by dropping a free-falling steel-weight (mass: 300 kg) from a prescribed height onto the center of the slab only once. And the impact velocity of the weight used in this analysis was varied from 5.0 to

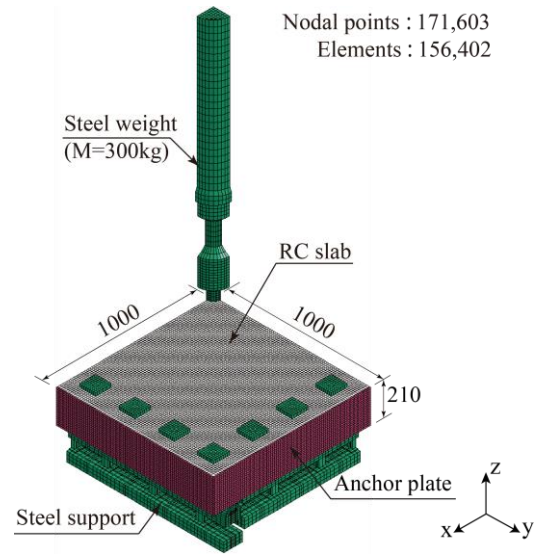


Fig. 2 Finite element models of slabs

6.5 m/s. The falling-weight was made of a steel solid cylinder of 1.4 m height and the striking part is 90 mm in diameter as shown in the photo 1. The impacting face was tapered with a height of 2 mm to prevent one-sided contact.

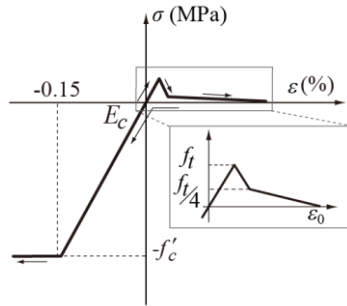
As shown in the photo 1, the RC slab was simple supported on the supporting points and fixed through bolts and nuts to prevent the ends of slab lifting off. And it was close to the pin support at the bottom of supporting apparatus, which are able to rotate freely while restraining movement of the slab.

In this experiment, the measurement items were: 1) the impact force P measured by using a load-cell that was installed in the weight, 2) the total reaction force R (hereinafter, reaction force) estimated by measuring load-cells installed in supporting apparatus, and 3) the deflection of the lower surface at the loading point (hereinafter, deflection) by using non-contact laser type linear variable displacement transducers. And the crack patterns on the bottom surface and central section surface at the loading point of the slab were also sketched after the experiment.

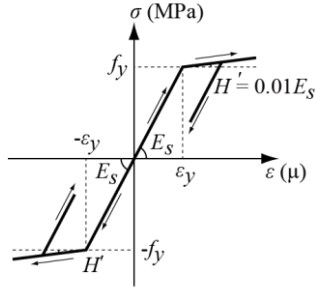
3. OVERVIEW OF NUMERICAL ANALYSIS

3.1 FE model

Figure 2 shows the finite element model of four-side supported RC slab used in this study. Here, due to the symmetry, only one-quarter of RC slab including the striker and supporting apparatus was modeled. In the model, all the elements were modeled by using eight-node solid elements with one integration point. And, the main rebars were simplified as square cross sections, which have same cross-section area as the nominal section area of rebars. In this study, to reproduce cracks clearly, a mesh size smaller than aggregate size of the concrete was adopted. Mesh size of FE model was approximately $12.5 \times 12.5 \times 10$ mm.



(a) Concrete



(b) Reinforcement

Fig. 3 Stress-strain relations of materials

Regarding of the boundary condition of FE model, the displacement in the normal direction of the symmetry surface was restrained, and only rotation at the bottom of the supporting apparatus was allowed corresponding to experimental conditions. Contact surfaces between concrete and reinforcements, and between concrete and anchor plate were assumed to be perfectly bonded to each other. The contact surface between the impact surfaces of concrete and weight, and between concrete and supporting apparatus including bolts and nuts were defined so as to allow contact or detach or slide to each other. In this analysis, Coulomb friction was adopted for friction model. And friction factor of the contact surface was assumed to be 0.2 based on pre-analysis results.

The impact load was applied by inputting an initial velocity for all the elements of the falling weight placed in the contact with RC slab. In this study, four analysis cases were conducted, in which the initial impact velocity of $V = 5.0, 5.5, 6.0,$ and 6.5 m/s were considered. Damping factor was assumed as $h = 5\%$ for the fundamental natural frequency of the vertical vibration mode based on the pre-analysis results [4]. And gravity was taken into consideration in this FE model.

3.2 Material models

In this study, to simulate actually the punching shear cracks of the RC slab, the erosion technique was introduced. Meanwhile, with the introduction of the concept of erosion, a cut-off model (MAT_14) for the tension side of concrete used by previous studies [4] cannot better simulate the punching shear failure shape of RC slab under impact loading. That is may be due to that the tension softening behavior of concrete element

after cracking is not considered. Therefore, a concrete model considering tension softening after cracking were applied in this analysis. And the suitable erosion values are determined based on a sensitivity analysis as presented specifically in Section 4.1.

Figure 3 shows the stress-strain relationships of concrete and rebars used in this study. The constitutive law model for each material was briefly described below.

(1) Concrete

Figure 3 (a) shows stress-strain relationships for concrete. The Winfrith Concrete model is used for the material model for concrete, which consider tension softening and strain rate effects [5]. For the compression side, a bilinear elasto-plastic model was applied, and concrete was yielded at 0.15 % strain. The yield stress of concrete was equal to the compressive strength f'_c obtained from the static test results as shown in the Table 1. And, yielding of concrete was evaluated based on the Ottosen shear failure surface [5].

For the tension side, a trilinear model was applied. In this model, after the equivalent principal stress reaches the tensile strength f_t , it decreases to $f_t/4$, and then the slope decreases gradually until the stress takes as zero as shown in Fig. 3(a). The tensile strength was set to be 1/10 of the compressive strength. The density ρ_c and Poisson's ratio ν_c were assumed as $\rho_c = 2.35 \times 10^3$ kg/m³ and $\nu_c = 0.167$, respectively. The strain softening behaviors [5] in the tension side were determined by the fracture energy G_F (energy per unit area dissipated in opening crack), which was calculated based on the Japan concrete design standard [6], as shown in the following equation.

$$G_F = 10 (d_{\max})^{1/3} \cdot (f'_c)^{1/3} \quad (\text{N/m}) \quad (1)$$

Where,

d_{\max} : maximum aggregate size (= 25mm)

f'_c : compressive strength of concrete (N/mm²)

In LS-DYNA code, the configuration of the tension softening including ϵ_0 was automatically determined by inputting the value of G_F . ϵ_0 was depended on the size of FE mesh, which was about 0.01 in this FE model.

(2) Reinforcement

The stress-strain relationships for reinforcements shown in Figure 3 (b). The Plastic_Kinematic model (MAT_003) was used for main rebars, in which an isotropic elasto-plastic hardening model considering plastic hardening modulus was applied. The plastic hardening modulus H' was assumed to be 1 % of elastic modulus E_s . Yielding of main rebars was evaluated following the von Mises's yield criterion. The yield stress f_y of the main rebars was obtained from the coupon test. Density ρ_s , Young's modulus E_s , and Poisson's ratio ν_s of the main rebars were assumed as $\rho_s = 7.85 \times 10^3$ kg/m³, $E_s = 206$ GPa, and $\nu_s = 0.3$, respectively.

(3) Falling-weight, supports, and anchor plate

For the falling-weight, supporting apparatus, and anchor plate, these were assumed as elastic bodies according to the experimental observations because no plastic deformation was observed in the experiment.

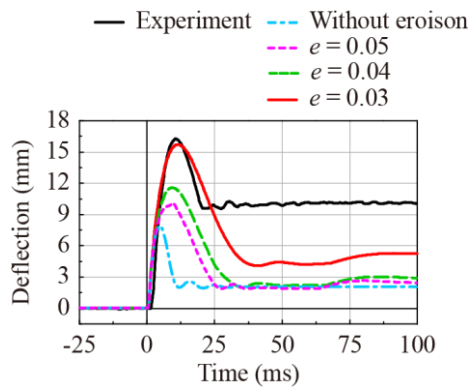


Fig. 4 Time histories of deflection for various erosion value ($V = 6.5\text{m/s}$)

Material properties: Young's modulus E_s and Poisson's ratio ν_s were set using the nominal value of steel ($E_s = 206\text{ GPa}$, $\nu_s = 0.3$). The density ρ_s was assumed as $\rho_s = 7.85 \times 10^3\text{ kg/m}^3$ for the supporting apparatus and anchor plate. The density of the falling weight was evaluated by dividing mass (300 kg) by volume of FE model.

4. NUMERICAL RESULTS AND DISCUSSIONS

4.1 Effect of erosion value

Here, to investigate the effect of erosion value on punching shear failure of the RC slab, a sensitivity analysis was conducted for the slab in which the punching shear failure was observed in the experiment. And the erosion value for maximum principal strain was applied with various values from 0.03 to 0.05 based on the literature study and preliminary analysis [7].

Figure 4 shows comparisons of time histories of deflections of the lower surface at the loading point among numerical results for various erosion value e and experimental results under impact velocity $V = 6.5\text{ m/s}$. In this figure, the origin of the time axis was taken as the time when the falling weight had just impacted onto the upper surface of the slab.

From the figure, it is observed that: 1) erosion value has significant effect on time histories of the deflection; 2) the maximum deflection was increased with a decrease of erosion value; and 3) residual deflections obtained from the numerical analyses were smaller than those of the experimental results; 4) in the case of the erosion value $e = 0.03$, the residual deflection may be larger than in the other analysis cases, because the stiffness of the RC slab is decreased by the removal of more concrete elements; and 5) in the case of erosion value $e = 0.03$, maximum deflection and time duration of main part were similar to those of experimental results.

From above results, it is clarified that erosion value has significant effect on impact resistant behavior of the RC slab and it can be better evaluated with erosion value $e = 0.03$ under the impact velocity $V = 6.5\text{ m/s}$. And, the applicability of the proposed condition will be investigated comparing with the experimental results for various impact velocity in the next section.

4.2 Time histories of impact force, reaction force, and deflection

Figure 5 shows the comparisons of time histories of impact response waves for impact velocity $V = 5.0, 5.5, 6.0, 6.5\text{ m/s}$ between experimental results and numerical ones with erosion value $e = 0.03$.

Figure 5 (a) shows comparisons of the time histories of impact force between numerical results and experimental results during a 20 ms time interval from the beginning of impact for all cases. From these figures, it is observed that: 1) configurations of time history of impact forces were composed of the first wave with large amplitude and short time duration; 2) maximum impact force was increased with an increment of impact velocity; and 3) maximum impact forces obtained from numerical results were smaller than those of experimental ones, however, configurations of time histories were in good agreement with experimental results for all cases.

Figure 5 (b) shows comparisons of the time histories of reaction force for a 40 ms time interval from the beginning of impact. From these figures, it is observed that: 1) configurations of time history of the reaction force were composed of the half sine wave with large amplitude and damping free vibration after that; 2) maximum reaction force obtained from numerical results were bigger than those of experimental results; 3) time duration of the main part obtained from the numerical results were shorter than those of experimental ones.

Figure 5 (c) shows comparisons of the time histories of the deflection of the lower surface at the loading point for a 200 ms time interval from the beginning of impact for all cases. From these figures, it is observed that: 1) the deflection reached a maximum value at an elapsed time of about 10 ms from the beginning of impact, and after that the slab was under damping free vibration; 2) maximum and residual deflections were increased with an increase of impact velocity, especially in the case of impact velocity $V = 6.5\text{ m/s}$, the deflection was increased rapidly that due to punching shear failure was occurred.

From the comparison between experimental and numerical results, it is observed that: 1) configuration of the time history of deflection was almost similar to each other; 2) maximum deflection obtained from numerical results were almost similar to those of experimental results for all cases; 3) in the case of impact velocity $V = 5.0, 5.5\text{ m/s}$, residual deflections obtained from numerical results were similar to those of experimental results; and 4) on the other hand, in the case of impact velocity $V = 6.0, 6.5\text{ m/s}$, residual deflections obtained from numerical results were smaller than those of experimental ones

4.3 Crack patterns on the bottom-surface

Figure 6 shows comparisons of crack patterns on the bottom-surface of the slab after the test between numerical and experimental results for all cases with erosion value $e = 0.03$. In the model, the cracks were visualized and were displayed in the black lines as shown in the figure.

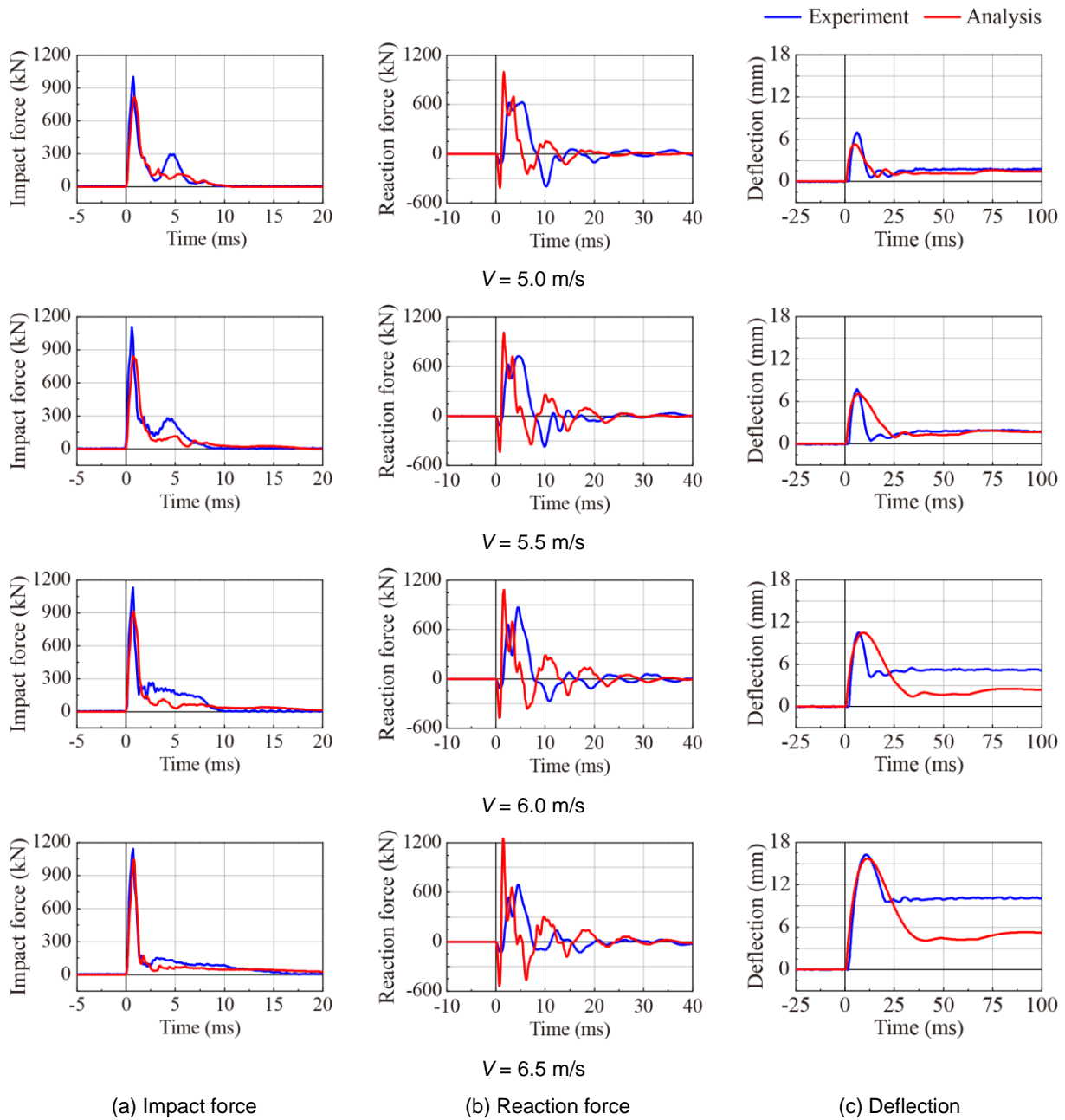


Fig. 5 Comparisons of impact response waves under various impact velocity

From the experimental results, it is shown that: 1) the crack pattern was composed of the circular-shaped cracks due to punching shear failure and the diagonal cracks from the center to the corner; 2) the areas of the circular-shaped cracks were more generated with an increment of impact velocity.

Comparing crack patterns between numerical and experimental results, it is observed that: 1) crack patterns obtained from numerical analysis tend to be undervalued than those of experimental results for all cases; 2) however, the circular-shaped cracks and diagonal cracks can be approximately better simulated.

4.4 Crack patterns on the central section surface

Figure 7 shows comparisons of crack patterns on the central section surface at the loading point of the slab between numerical and experimental results for all cases with erosion value $e = 0.03$.

From these figures, it is shown that: 1) the crack pattern was composed of 45-degree punching shear cracks from the load points to reinforcing bars arranged in the lower part of the slab; 2) the cracks were more generated with an increment of impact velocity, crushing of concrete was occurred on the top surface of slab near the loading point in the case of impact velocity $V = 6.5$

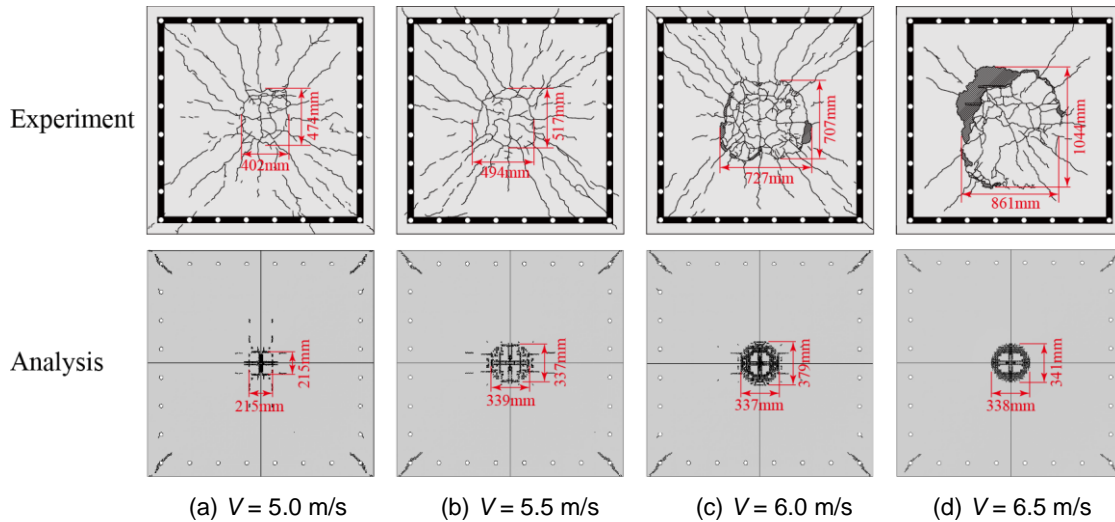


Fig. 6 Comparisons of crack patterns on the bottom side of slab

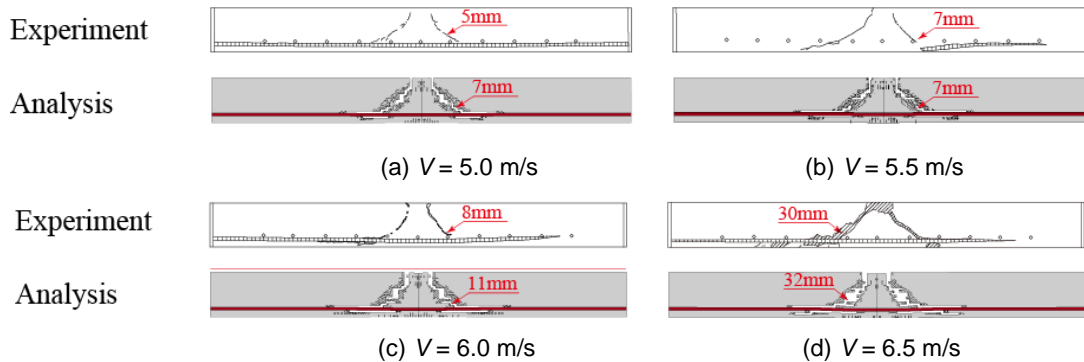


Fig. 7 Comparisons of crack patterns of central section surface of slab

m/s; and 3) the 45-degree punching shear cracks and the crack width can be better simulated use this analysis method with the suitable erosion value.

5. CONCLUSIONS

- (1) The erosion value has significant effect on the impact behaviors of slab with local punching shear failure under low-speed impact velocity;
- (2) Use the proposed analysis method, maximum impact force, and maximum deflections can be almost predicted; and
- (3) Circular-shaped cracks and diagonal cracks on the bottom-surface and 45-degree punching shear cracks on the central section surface of the slab can be better simulated.

REFERENCES

- [1] F. Delhomme., M. Mommessin., J.P. Mougin., and P. Perrotin., "Behavior of a Structurally Dissipating Rock-shed: Experimental Analysis and Study of Punching Effects," *International Journal of Solids and Structures*, Vol. 42, Issue. 14, 2005, pp. 4204-4219.
- [2] Kishi, N., Mikami, H., Kurihashi, Y., "A Proposal of Design Procedures for RC Slabs with Various Supporting Conditions and Thicknesses under Falling-weight Impact Loading," *Journal of Structural Engineering*. Vol. 59A, 2013, pp. 1025-1036. [in Japanese]
- [3] Yamaguchi, S., Kohata, Y., Komuro, M., and Kishi, N., "Falling-weight impact test for full-scale RC type rock-shed with sand cushion," *Proc. of the JCI*, Vol. 36, No. 2, 2014, pp. 553-558. [in Japanese]
- [4] Zheng, D., Komuro, M., Kishi, N., and Kurihashi, Y., "Dynamic Response Analysis of RC Slabs with Various Support Conditions under Impact Loading," *Proc. of the JCI*, Vol. 40, No. 2, 2018, pp. 685-590.
- [5] L. Schwer, "The Winfrith Concrete Model: Beauty or Beast? Insights into the Winfrith Concrete Model," *Schwer Engineering & Consulting Services*, 8th European LS-DYNA Users Conference, Strasbourg, 2011.
- [6] *Standard Specifications for Concrete Structures-2012*, Design. JSCE.,2012, pp. 38.
- [7] Thai, D. K., and Kim, S. E., "Numerical Simulation of Pre-stressed Concrete Slab Subjected to Moderate Velocity Impact Loading," *Engineering Failure Analysis*, Vol. 79, 2017, pp. 820-835.